

Stability, coherent spiking and synchronization in noisy excitable systems with coupling and internal delays

Igor Franović^a, Kristina Todorović^b, Nebojša Vasović^c, Nikola Burić^{d,*}

^a Faculty of Physics, University of Belgrade, PO Box 44, 11001 Belgrade, Serbia

^b Department of Physics and Mathematics, Faculty of Pharmacy, University of Belgrade, Vojvode Stepe 450, Belgrade, Serbia

^c Department of Applied Mathematics, Faculty of Mining and Geology, University of Belgrade, PO Box 162, Belgrade, Serbia

^d Scientific Computing Lab., Institute of Physics, University of Beograd, PO Box 68, 11080 Beograd-Zemun, Serbia

ARTICLE INFO

Article history:

Received 7 November 2013

Received in revised form 11 February 2014

Accepted 17 February 2014

Available online 26 February 2014

Keywords:

Time-delay

Noise

Coherent spiking

ABSTRACT

We study the onset and the adjustment of different oscillatory modes in a system of excitable units subjected to two forms of noise and delays cast as external or internal according to whether they are associated with inter- or intra-unit activity. Conditions for stability of a single unit are derived in case of the linearized perturbed system, whereas the interplay of noise and internal delay in shaping the oscillatory motion is analyzed by the method of statistical linearization. It is demonstrated that the internal delay, as well as its coaction with external noise, drive the unit away from the bifurcation controlled by the excitability parameter. For the pair of interacting units, it is shown that the external/internal character of noise primarily influences frequency synchronization and the competition between the noise-induced and delay-driven oscillatory modes, while coherence of firing and phase synchronization substantially depend on internal delay. Some of the important effects include: (i) loss of frequency synchronization under external noise; (ii) existence of characteristic regimes of entrainment, where under variation of coupling delay, the optimized unit (noise intensity fixed at resonant value) may be controlled by the adjustable unit (variable noise) and vice versa, or both units may become adjusted to coupling delay; (iii) phase synchronization achieved both for noise-induced and delay-driven modes.

© 2014 Elsevier B.V. All rights reserved.

1. Introduction

Generation of different oscillatory modes and their mutual adjustment constitute the basic paradigm behind the local and cooperative dynamics in a wide variety of biological and inorganic systems. Modeling complex multi-scale systems often consists in singling out the components showing typical and well controllable behavior into a few selected degrees of freedom, whereas their interactions incorporate explicit time-delays and different forms of noise. The stochastic component is intended to approximate variations within the embedding environment, as well as the fluctuations due to processes taking place at smaller spatial and temporal scales. The delays typically emerge due to complexity of interactions. In particular, the origin of delay between a sending and a receiving element may be linked to (i) intrinsic times of signal generation in the sending element, (ii) the finite propagation velocity of signals, and (iii) the latency in signal processing of the receiving element [1]. By their characteristic spatial and time-scales, the delays and sources of noise can naturally be associated with the

* Corresponding author. Tel.: +381 11 3160260; fax: +381 11 3162190.

E-mail address: buric@ipb.ac.rs (N. Burić).

degrees of freedom pertaining to a single unit (“internal” noise and delays) or those related to the interactions between the units (“external/interaction” noise and delays).

The existence of multiple noises and delays, together with the vast separation of characteristic time scales of the underlying processes, are inevitable features accompanying the modeling of many different biological systems. While the mere presence of these ingredients may be thought of as universal, the prevalence of one type of noise/delay over the other in regard to impact on the system dynamics is an individual feature of any particular system. For instance, the external (synaptic) noise is the dominant factor in the evolution of neuronal systems [2], whereas the internal (biochemical) noise, arising due to small numbers of reactants’ molecules [3], is likely the most prominent form of noise for the dynamics of gene expression regulatory networks [4,5]. Nonetheless, in neuronal systems the conduction delays of type (ii) are manifested more strongly than the delays of type (iii), while in gene networks the coupling delays of types (i) and (iii) occur naturally due to multistage synthesis of the reactants and the complex kinetics of intercellular signaling [5,6]. Regarding the photosynthesis and the related photo-respiration cycle, it has been indicated that the primary stochastic component comes from biochemical noise due to small numbers of reacting molecules [7], whereas the delay may be associated with the multistage assembly of reactants, the processes one would expect to naturally involve memory effects. Notably, there is ample evidence that in many biological systems noise and delay, alone or combined, play a significant role. Apart from the well known impact of these ingredients on neuronal systems [8–12], it has also been found that noise substantially affects the gene expression [13–15]. Also, the delayed negative feedback loops induce oscillations in gene transcription networks [16,6], whereas the interplay of randomness and delay has been demonstrated to accelerate signaling in genetic pathways [17,18,6]. As for photosynthesis, it has been suggested that the optimal amount of noise may enhance efficiency of energy transfer at certain stages of the process [19].

In this paper, the aim is to study in detail the interplay of internal and interaction delays and noise on formation and adjustment of oscillatory modes. This issue is especially intricate if the system is not made up of autonomous oscillators, but rather of excitable units [20]. Excitability rests on the point that equilibrium is poised close to a bifurcation toward periodic activity, whereby a unit may produce oscillations under permanent perturbation. If additional ingredients, such as delays, lead to coexistence of equilibrium and certain oscillatory states, then it becomes interesting to examine how excitability feature is modified due to multistability. Note that the body of work referring to models involving coaction of noise and delays is significantly less compared to those where either of them acts alone. Reluctance to consider nonlinear stochastic models with delays is mainly caused by the fact that the underlying systems of nonlinear stochastic delay-differential equations (SDDEs) are rarely tractable analytically [21,22].

The research here is focused on interaction of stochastic excitable units, whose dynamics is influenced by the coupling and intrinsic delays. We consider a pair of Fitzhugh–Nagumo (FHN) elements, which may be viewed as a basic motif of some complex network. While two distinct forms of perturbation are included as additive noise within the fast and slow subsystems, the model also features two types of delays, one incorporated into the coupling terms and the other related to the recovery mechanism of individual units. Our main goal is to study the particular roles and the co-effects of internal and interaction noise and delays on stability of equilibrium and the onset of different oscillatory modes, further examining regularity of spiking and certain forms of coordinated behavior cast within the framework of stochastic synchronization. Note that the combined effects of two types of noise on a single unit have been considered in [23,24], whereas synchronization of interacting stochastic units in the absence of coupling delays has been analyzed in [25,26]. On the other hand, the results on bifurcations and stability of exact synchronization in the unperturbed system admitting interaction delays have been reported in [27]. Compared to these studies, the novel points here concern (i) the presence of internal delays in each unit, (ii) application of several analytical techniques on the underlying model, including calculation of the stability conditions for the linearized system under perturbation and the method of statistical linearization, as well as (iii) putting emphasis on the competition between the noise-induced and delay-driven oscillatory modes, especially in terms of how it is reflected on the frequency and phase synchronization between the units.

The paper is organized as follows. Section 2 concerns the details of the model, specifying the background and the role of the introduced stochastic terms and delays. Section 3 provides the analysis on stability of a single unit. Apart from considering the local and global bifurcations controlled by intrinsic delay in the deterministic system, we derive the appropriate Fokker–Planck equation and determine stability conditions for the first two moments of the linearized system under perturbation. Method of statistical linearization is applied to study how coaction of noise and delay affects the unit’s oscillatory motion. In Section 4, a pair of interacting units is approached by performing bifurcation analysis for the noiseless case, which demonstrates the prevalence of bistable regimes, either between equilibrium and the oscillatory states or between the different oscillation modes. Section 5 contains numerical results, intended to gain insight into the competition between the delay- and noise-driven modes. The issues of spiking coherence and stochastic synchronization are systematically examined under variation of delays, while letting the noise amplitudes take values below, about and above the resonant ones. Concluding remarks are provided in Section 6.

2. Details of the applied model

We consider a couple of identical excitable elements subjected to two types of noise and delay. In its most general form, the model dynamics is given by

$$\begin{aligned} \epsilon dx_i &= [x_i - x_i^3/3 - y_i(t - \tau_{in})]dt + \sqrt{\epsilon} \sqrt{2D_1^i} dW_1^i + c[x_j(t - \tau_{ex}) - x_i(t)]dt, \\ dy_i &= (x_i + b)dt + \sqrt{2D_2^i} dW_2^i, \end{aligned} \quad (1)$$

where $i, j \in \{1, 2\}$, $i \neq j$ denote unit indices. Parameter $\epsilon = 10^{-2}$ is set to a small value to ensure a sharp time scale separation between the activator variables x_i and the respective recovery variables y_i . In the context of neuroscience, FHN model is regarded as phenomenological, but an analogy may still be drawn between the behavior of the fast variables and the evolution of membrane potential [20]. One may further compare the action of slow variables to a group of complementing relaxation processes, where the most salient is driven by the potassium gating channels. The terms dW_1^i and dW_2^i stand for the stochastic increments of the independent Wiener processes. Their expectations and correlations satisfy $\langle dW_k^i(t) \rangle = 0$ and $\langle dW_k^i(t) dW_l^j(t') \rangle = \delta_{kl} \delta_{ij} dt$, having introduced $k, l \in \{1, 2\}$ to distinguish whether noise acts within the fast or slow subsystem of each unit. Extending the above arguments, the role of stochastic terms in x_i dynamics may be compared to synaptic noise, made up of random inputs continuously impinging on any given cell from its peer neurons. Note that the synaptic noise constitutes by far the most important noise source in cortical neurons, arising due to the combination of sustained irregular activity and the typically high connectivity of units [2]. As for the stochastic terms in y_i dynamics, one may conditionally interpret them as thermal noise triggering the random conformation changes of ion-gating channels in the neuron's semi-permeable membrane [23,28]. Since the random fluctuations introduced into fast-variable subsystems may be attributed to the effects of surrounding, whereas the stochastic component in the y_i dynamics may be associated with the intra-unit sources, in the rest of the paper we refer to them as *external* and *internal noise* [2], respectively.

The form of interaction between the excitable units depends on the particular physical system the model refers to. The most elementary interaction is given by the linear coupling, which in neuronal modeling conforms to electrical synapse. The difference between the characteristic time-scale of $x_i(t)$ and the one at which the interactions take place justifies the assumption that the coupling terms should include an explicit time-delay τ_{ex} . The latter corresponds to the time it takes an excitation to travel between the two connected units at finite propagation speed. Parameter c characterizes the coupling strength. Following a more detailed analysis of (1), one may argue that there are three qualitatively different domains of c values. For sufficiently small c , the units act as if they were independent. Nonetheless, in the noiseless and delay-free case, for comparably large c the total system behaves as a single multidimensional oscillator. Adding noise and delay then induces only quantitative changes in the properties of the multidimensional oscillations. Therefore, c is fixed to an intermediate value $c = 0.1$, so that variation of delay and noise may introduce qualitative changes in the system dynamics.

Our model also features the intrinsic time delay τ_{in} , which is an order of magnitude smaller than the characteristic time-scale set by $y_i(t)$. Its role is to modify the relaxation process by influencing the refractory stage after a spike has been elicited. In terms of neuronal modeling, if the analogy between the dynamics of $y_i(t)$ and the ion-gating channels is accepted, one should also appreciate the point that the channels themselves are composed of subunits which have to act in concert to reach the open state. The time necessary to do so, accounted for by τ_{in} , effectively becomes prevalent in the “slope” describing recovery of $x_i(t)$ to the rest state. In a broader sense, τ_{in} specifies an intermediate time-scale, nested between the ones defined by $x_i(t)$ and $y_i(t)$. Such a setup is not unlike the already considered scenario where the FHN units are exposed to colored noise [29], whose correlation time lies between $\mathcal{O}(\epsilon)$ and $\mathcal{O}(1)$. Note that though the internal delay and internal noise may be conditionally associated with the dynamics of ion-channel gating, the mechanisms contributing them are independent. To clarify this, one may invoke a comparison between a certain system influenced by inherent randomness, e.g. internal noise, and a system where the stochastic component coexists with the memory effects. While the former would be described by a set of stochastic differential equations, the dynamics of the latter would be represented by a system of stochastic delay-differential equations, where the terms accounting for the noise and delay are not related.

To briefly explain excitability, let us temporarily confine the discussion to an isolated unit with $\tau_{in} = 0$. Excitability rests on the proximity of equilibrium to a bifurcation toward the oscillatory state. FHN model belongs to type II excitability class, which implies that the unit undergoes direct supercritical Hopf bifurcation at the critical threshold [20]. In our case, the bifurcation parameter is b , whose critical value is given by $|b| = 1$: for $|b| > 1$ the unit lies at equilibrium, whereas for $|b| < 1$ there exists a limit cycle. Since (1) is invariant under the transformation $(x_i, y_i, b) \rightarrow (-x_i, -y_i, -b)$, it suffices to consider only the case $b > 0$. For a slightly supra-critical b , say $b = 1.05$, the value fixed throughout the paper, a unit is in the excitable regime: under weak perturbation, it rapidly relaxes back to equilibrium, but an adequate perturbation may elicit a spike, associated with the representative point making a large excursion in phase space before equilibrium is regained.

In model (1), the oscillation modes can be induced by any of the time delays or by any of the noise terms. It is well known that τ_{ex} introduces oscillatory motion via the local Hopf or by the global fold-cycle bifurcation, whereby a similar point will be shown for τ_{in} . The modes derived from these two scenarios are rather different. Nonetheless, under permanent perturbation, excitable units generate oscillations, which can become coherent at an optimal noise intensity. Two profoundly distinct resonance mechanisms have been established for the additive noise influencing either the activator or the recovery variable. In case of coherence resonance (CR), occurring under internal noise, the stochastic limit cycle is just the precursor of the deterministic one [30,31]. Its phase portrait is akin to the those found in relaxation oscillators, with the two pieces of slow motion $\mathcal{O}(1)$ connected by the two fast transients $\mathcal{O}(\epsilon)$, see Fig. 1(a). The resonance mechanism is based on a trade-off between the durations of the activation and the relaxation times. Nevertheless, in case of self-induced stochastic resonance (SISR), taking place under external noise, the phase portrait of the stochastic cycle is substantially different from the one found in the supercritical deterministic system [31,24], especially with respect to escape from the refractory and the spiking

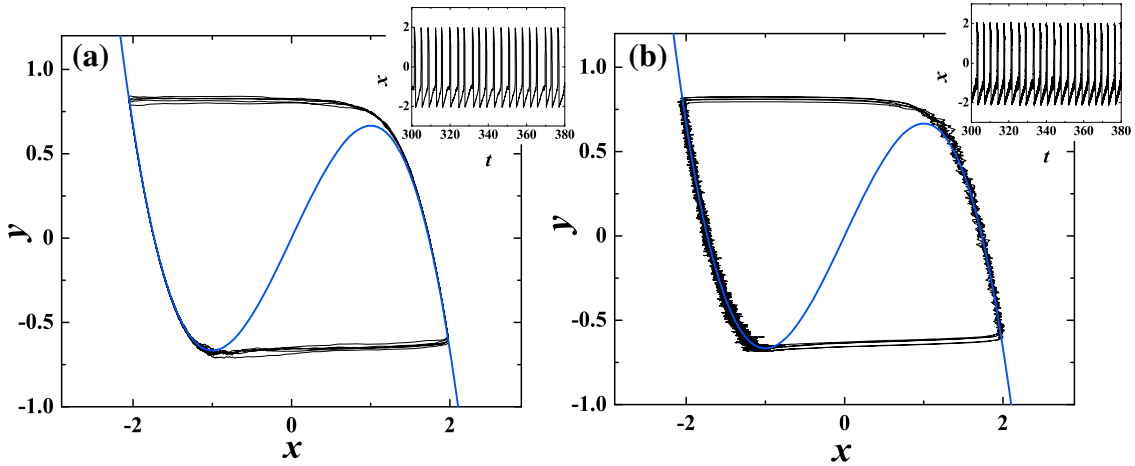


Fig. 1. (a) and (b) show phase portraits typical for oscillations induced by internal and external noise, respectively. The noise intensities $D_2 = 0.0021$ and $D_1 = 0.0009$ are close to resonant values. In the CR case, the orbit follows the refractory and the spiking branch given by the activator nullcline $x - x^3/3 = y$, whereas the points of escape from the branches approximately coincide with the knees $(x_l, y_l) = (-1, -2/3)$ and $(x_r, y_r) = (1, 2/3)$ of the nullcline. Under the SISr scenario, the stochastic limit cycle is not the precursor of the deterministic one. In the insets are displayed the corresponding $x(t)$ series.

branches, cf. Fig. 1(b). The resonance mechanism is much more intricate, and is based on keeping the phase point frustrated at the refractory branch so it can never reach the branch’s knee. In qualitative sense, note that the action of internal noise has a clear interpretation, as it modifies the position of the recovery variable’s nullcline, given by $x_i = -b$. This can make the equilibrium unstable, temporarily pushing the system over the critical threshold. Role of external noise cannot be interpreted in a similar fashion.

Given the arguments above and the stated objective to understand the interplay of noise, τ_{ex} and τ_{in} on systems of excitable units, we treat the cases with external and internal noise separately. This is done so because otherwise the co-effects of noise terms and the co-effects of noise and delays become rather difficult to distinguish.

3. Analysis of the single unit’s dynamics

3.1. Derivation of the Fokker–Planck equation

Having made an overview of the dynamics exhibited by a single unit under the influence of noise, let us turn to the analysis of the co-effects of noise and the internal delay. Our intention is to first illustrate the obstacles one is faced with when attempting to tackle this problem via the Fokker–Planck formalism. To this end, we derive the appropriate Fokker–Planck equation assuming the general case of a unit subjected to both external and internal noise ($c = 0, D_1 > 0, D_2 > 0$). Since system (1) features only additive noise, the result is independent on whether Itô or Stratonovich interpretation has been adopted [32]. To begin with, note that the probability distribution of x and y is defined by $p(x, y, t) = \langle \delta[x(t) - x] \delta[y(t) - y] \rangle$, where $\langle \cdot \rangle$ denotes averaging over the realizations of the stochastic processes, and the unit index has been dropped for simplicity. Taking the time derivative of the above expression and using the properties of the Dirac delta function, one arrives at

$$\begin{aligned} \frac{\partial}{\partial t} p(x, y, t) = & -\frac{\partial}{\partial x} \langle \delta[x(t) - x] f(x(t), y_{\tau_{in}}) \rangle \langle \delta[y(t) - y] \rangle - \frac{\partial}{\partial y} \langle \delta[y(t) - y] \rangle \langle \delta[x(t) - x] g(x(t)) \rangle \\ & - \sqrt{\frac{2D_1}{\epsilon}} \frac{\partial}{\partial x} \langle \delta[x(t) - x] \xi_1(t) \rangle \langle \delta[y(t) - y] \rangle - \sqrt{2D_2} \frac{\partial}{\partial y} \langle \delta[y(t) - y] \xi_2(t) \rangle \langle \delta[x(t) - x] \rangle, \end{aligned} \tag{2}$$

where the notation $y_{\tau_{in}} \equiv y(t - \tau_{in})$, $\xi_1(t) = dW_1/dt$, $\xi_2(t) = dW_2/dt$, as well as $f(x(t), y_{\tau_{in}}) = [x(t) - x^3(t)]/3 - y(t - \tau_{in})/\epsilon$, $g(x(t)) = x(t) + b$ has been introduced for shorthand. The averages containing stochastic terms can be handled by the Furutsu–Novikov formula [21], which here results in

$$\langle \delta[x(t) - x] \xi_1(t) \rangle = \int_0^t \langle \xi_1(t) \xi_1(t') \rangle \left\langle \frac{\delta\{\delta[x(t) - x]\}}{\delta \xi_1(t')} \right\rangle dt' = \left\langle \frac{\delta\{\delta[x(t) - x]\}}{\delta \xi_1(t)} \right\rangle \tag{3}$$

and the analogous relation for $\langle \delta[y(t) - y] \xi_2(t) \rangle$, having applied $\langle \xi_1(t) \xi_1(t') \rangle = \delta(t - t')$ and $\langle \xi_2(t) \xi_2(t') \rangle = \delta(t - t')$. Employing again the properties of the delta function, the functional derivative in (3) may be written as

$$\left\langle \frac{\delta\{\delta[x(t) - x]\}}{\delta\xi_1(t)} \right\rangle = \left\langle -\frac{\partial}{\partial x} \delta[x(t) - x] \frac{\delta x(t)}{\delta\xi_1(t)} \right\rangle, \quad (4)$$

with the similar relation obtained for $\left\langle \frac{\delta\{\delta[y(t) - y]\}}{\delta\xi_2(t)} \right\rangle$. From (1) it follows that $\frac{\delta x(t)}{\delta\xi_1(t)} = \sqrt{\frac{2D_1}{\epsilon}}$ and $\frac{\delta y(t)}{\delta\xi_2(t)} = \sqrt{2D_2}$. Knowing that the average $\langle \delta[x(t) - x] \rangle$ may be calculated as $\langle \delta[x(t) - x] \rangle = \int_{-\infty}^{\infty} \int_{-\infty}^{\infty} \delta[x(t) - x] p(x, y, t) dx dy$, one finds

$$\langle \delta[x(t) - x] \xi_1(t) \rangle = -\sqrt{\frac{2D_1}{\epsilon}} \frac{\partial}{\partial x} p(x, y, t), \quad (5)$$

and by the same token,

$$\langle \delta[y(t) - y] \xi_2(t) \rangle = -\sqrt{2D_2} \frac{\partial}{\partial y} p(x, y, t). \quad (6)$$

The results so far refer to the final two terms on the right side of (2). Regarding the first term, by using the law of total expectation, it follows that

$$\langle \delta[x(t) - x] \delta[y(t) - y] f(x(t), y_{\tau_{in}}) \rangle = \iiint \delta[x(t) - x] \times \delta[y(t) - y] [(x(t) - x^3(t)/3 - y_{\tau_{in}})/\epsilon] p(x, y, y_{\tau_{in}}) dx dy dy_{\tau_{in}}. \quad (7)$$

Under general conditions, one cannot assume the statistical independence between $x(t)$ and $y(t)$ on one hand and $y(t - \tau_{in})$ on the other. Therefore, the probability $p(x, y, y_{\tau_{in}})$ may only be written in the form $p(x, y, y_{\tau_{in}}) = p(y_{\tau_{in}} | x, y) p(x, y)$, where $p(y_{\tau_{in}} | x, y)$ presents the conditional probability of finding $y_{\tau_{in}}$ at the moment $t - \tau_{in}$, provided that $(x(t), y(t)) = (x, y)$. Inserting the expression for $p(x, y, y_{\tau_{in}})$ into (7), we find

$$\langle \delta[x(t) - x] \delta[y(t) - y] f(x(t), y_{\tau_{in}}) \rangle = p(x, y, t) \times \frac{1}{\epsilon} \left[x(t) - x^3(t)/3 - \int y_{\tau_{in}} p(y_{\tau_{in}} | x, y) dy_{\tau_{in}} \right], \quad (8)$$

where the last term on the right constitutes the so-called conditional drift [22,21,33]

$$\langle y_{\tau_{in}} | x(t), y(t) \rangle = \int y_{\tau_{in}} p(y_{\tau_{in}} | x, y) dy_{\tau_{in}} \quad (9)$$

emerging due to non-Markovian character of the SDDE system (1). Collecting the above results and substituting them into (2), we obtain the Fokker–Planck equation for a FHN unit subjected to external and internal noise, as well as internal delay

$$\begin{aligned} \frac{\partial}{\partial t} p(x, y, t) = & -\frac{1}{\epsilon} \frac{\partial}{\partial x} [x(t) - x^3(t)/3 - \langle y_{\tau_{in}} | x(t), y(t) \rangle] \times p(x, y, t) - \frac{\partial}{\partial y} [x(t) + b] p(x, y, t) + \frac{2D_1}{\epsilon} \frac{\partial^2}{\partial x^2} p(x, y, t) + 2D_2 \\ & \times \frac{\partial^2}{\partial y^2} p(x, y, t). \end{aligned} \quad (10)$$

The standard way to proceed would be to determine the stationary solution of (10), whereby the conditions for system's stability should be inferred by calculating the parameter values under which the stationary distribution can no longer be normalized [21]. The main obstacle for completing this task lies in the inability to resolve the conditional drift term (9) analytically, which forces us to explore other means of estimating the co-effects of noise and internal delay on stability of the stationary solution.

3.2. Deterministic system and stability of the linearized system under stochastic perturbation

To get a sense on the impact of τ_{in} on the dynamics of a single unit, we analyze its behavior in the deterministic case, obtained from (1) by setting $c = 0, D_1 = 0, D_2 = 0$. The index of the selected unit has again been dropped for simplicity. Stability of the stationary solution is determined by the roots of the characteristic equation. The first step in deriving the latter is to linearize the system describing the isolated unit around the fixed point $(x_0, y_0) = (-b, -b + b^3/3)$. Assuming that the deviations are of the form $\delta x(t) = Ae^{\lambda t}, \delta y(t) = Be^{\lambda t}$ and $\delta y(t - \tau_{in}) = Be^{\lambda(t - \tau_{in})}$, one arrives at a system of algebraic equations over the coefficients A and B . The condition for this system to possess a nontrivial solution is provided by the characteristic equation

$$\epsilon \lambda^2 - \lambda(1 - b^2) + e^{-\lambda \tau_{in}} = 0, \quad (11)$$

whose transcendental form reflects the presence of time delay in the unit's dynamics [34–36]. For the parameter values $(\epsilon, b) = (0.01, 1.05)$ kept throughout the paper, we have numerically found that the two complex-conjugate roots of (11) cross the imaginary axes at $\tau_{in}^H = 0.118$, which indicates the onset of a limit cycle via Hopf bifurcation. Note that the roots

of (11) obtained for small $\tau_{in}, \lambda_{\pm} = \frac{1 + \tau_{in} - b^2 \pm \sqrt{(1 + \tau_{in} - b^2)^2 - 4\epsilon}}{2\epsilon}$, imply that the addition of intrinsic delay drives the system away from the critical threshold of the Hopf bifurcation controlled by the parameter b , meaning that a unit becomes less excitable.

Nevertheless, it turns out that the complete knowledge on the system's behavior with τ_{in} cannot be gained by performing just the local bifurcation analysis. Apart from the Hopf bifurcation, τ_{in} gives rise to another oscillatory mode by inducing a

global (direct) fold-cycle bifurcation in which an unstable and a large stable limit cycle are born. This global event occurs around $\tau_{in}^{FC} = 0.106$, a value smaller than τ_{in}^H . Since the fold-cycle bifurcation does not affect the local stability of the fixed point, a deterministic unit exhibits bistability, i.e. coexistence between the equilibrium and the limit cycle within the interval $\tau_{in}^{FC} < \tau_{in} < \tau_{in}^H$. However, we also report on an interesting interplay between the local and the global bifurcation for $\tau_{in} > \tau_{in}^H$. It turns out that the incipient cycle, emerging around the position of the former equilibrium for $\tau_{in} = \tau_{in}^H$ grows only until colliding with the unstable cycle born in the global bifurcation. These two cycles get annihilated in an inverse fold-cycle bifurcation, such that the large cycle, created in the direct fold-cycle bifurcation at $\tau_{in} = \tau_{in}^{FC}$, remains as the only attractor. Phase portrait of the large cycle is substantially distinct from those of cycles emerging due to noise, cf. Fig. 2(a) and what is shown in Fig. 1(a) and (b). The apparent differences in the relaxation stage are consistent with the role of τ_{in} , as explained in Section 2.

Intuitively, adding external or internal noise to physical picture governed by τ_{in} could result in several effects. For $\tau_{in} < \tau_{in}^{FC}$, a coherent noise-driven mode will emerge at an optimal noise-intensity, whereas rare spiking or fast incoherent spiking will occur at small or large noise intensities, respectively. Within the interval $\tau_{in}^{FC} < \tau_{in} < \tau_{in}^H$, the system is likely to become monostable even for very small noise, because stability of equilibrium would be rather sensitive to its presence. The similar point on the loss of bistability also applies to τ_{in} values slightly above τ_{in}^H , where the deterministic system displays coexistence between a small and a large limit cycle. For any $\tau_{in} > \tau_{in}^{FC}$, under increasing noise one is likely to first encounter competition between the delay- and the noise-driven mode, whereas at some point, the stochastic component would overwhelm the deterministic one. We point out that the period of the mode elicited by τ_{in} is typically larger than the average ISI characterizing the noise-led oscillations, cf. $T = 4.44$ for the cycle in Fig. 2(a) vs $\langle T \rangle = 3.8$ for that in Fig. 1(a). This will prove useful in interpreting the outcome of the competition between the noise- and delay-driven modes later on.

Before considering the effects of perturbation on stability, we make a brief qualitative remark on the interplay of internal noise and τ_{in} . For small τ_{in} , one can expand the term $y(t - \tau_{in})$ to first order $y(t - \tau_{in}) \approx y(t) - \tau_{in} \frac{dy}{dt}$, which may be used to transform the equations for a single unit into

$$\begin{aligned} \epsilon dx &= (x - x^3/3 - y(t))dt + \tau_{in}(x(t) + b)dt + \tau_{in}\sqrt{2D_2}dW_2, \\ dy &= (x + b)dt + \sqrt{2D_2}dW_2, \end{aligned} \tag{12}$$

This reveals an interesting point that the co-effect of internal delay and internal noise may actually be treated by drawing an analogy to a delay-free system subjected to noise in both the slow and the fast variable, whereby the latter is an order of magnitude smaller than the former. Note that the system described by (12) can be fully analyzed within the Fokker-Planck formalism.

As a final point on the stability of a single unit, we discuss the stability of the system linearized around the stationary solution $(x_0, y_0) = (-b, -b + b^3/3)$ under stochastic perturbation [21,38,37]. Given that the perturbation is provided by the Gaussian distributed white noise with zero mean and a delta function autocorrelation, it is sufficient to consider the stability of the first $(\langle \delta x(t) \rangle, \langle \delta y(t) \rangle)$ and second moments $(\langle \delta x^2(t) \rangle, \langle \delta y^2(t) \rangle, \langle \delta x(t) \delta y(t) \rangle)$ of the solution [38,37], where $\delta x(t) = x(t) - x_0$ and $\delta y(t) = y(t) - y_0$. To derive the equations describing the dynamics of the first moments, one starts off from the linearized system

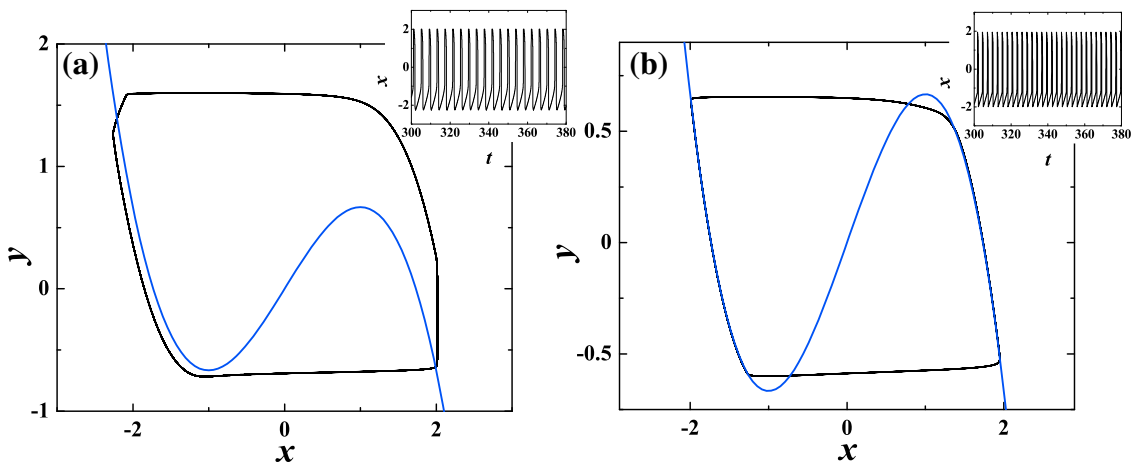


Fig. 2. (a) and (b) show phase portraits corresponding to limit cycles born in global fold-cycle bifurcations induced by τ_{in} and τ_{ex} , respectively. Note that the former does not follow the cubic nullcline during the declining stage of spike, whereas the latter's orbit involves escaping the slow branches before reaching the knees of the nullcline. In the insets are shown the corresponding $x(t)$ series. (a) is obtained for a single noiseless unit at $\tau_{in} = 0.4$, while (b) refers to a setup with interacting noiseless units for $(c, \tau_{ex}) = (0.1, 1.2)$.

$$\begin{aligned}d\delta x(t) &= \frac{1}{\epsilon}[(1-b^2)\delta x(t) - \delta y(t - \tau_{in})]dt + \sqrt{\frac{2D_1}{\epsilon}}dW_1(t), \\d\delta y(t) &= \delta x(t)dt + \sqrt{2D_2}dW_2(t).\end{aligned}\tag{13}$$

Carrying out integration from 0 to t , taking the expectation and finally differentiating with respect to t , from (13) we arrive at

$$\begin{aligned}d\langle\delta x(t)\rangle &= \frac{1}{\epsilon}[(1-b^2)\langle\delta x(t)\rangle - \langle\delta y(t - \tau_{in})\rangle]dt, \\d\langle\delta y(t)\rangle &= \langle\delta x(t)\rangle dt,\end{aligned}\tag{14}$$

which is completely analogous to the set of equations determining the stability of the unperturbed unit. Thus, stability of the first moments is readily solved by applying the results reached for the deterministic system.

As far as the equations governing the dynamics of the second moments are concerned, we begin the derivation by taking the Itô derivative [32,46] of $\delta x^2(t)$ and $\delta y^2(t)$. If the steps from above are repeated, using the linearized system (12) and the properties of the stochastic integrals in the Itô interpretation [32], one arrives at

$$\begin{aligned}\frac{d}{dt}\langle\delta x^2(t)\rangle &= \frac{2}{\epsilon}\left[(1-b^2)\langle\delta x^2(t)\rangle - \langle\delta x(t)\delta y_{\tau_{in}}\rangle + D_1\right], \\ \frac{d}{dt}\langle\delta y^2(t)\rangle &= 2\langle\delta x(t)\delta y(t)\rangle + 2D_2, \\ \frac{d}{dt}\langle\delta x(t)\delta y(t)\rangle &= \frac{1}{\epsilon}\left[(1-b^2)\langle\delta x(t)\delta y(t)\rangle - \langle\delta y(t)\delta y_{\tau_{in}}\rangle\right] + \langle\delta x^2(t)\rangle.\end{aligned}\tag{15}$$

Stability of the second-order moments can be analyzed by introducing the two-time correlation functions $C_{xx}(t, t') \equiv \langle\delta x(t)\delta x(t')\rangle$, $C_{yy}(t, t') \equiv \langle\delta y(t)\delta y(t')\rangle$ and $C_{xy}(t, t') \equiv \langle\delta x(t)\delta y(t')\rangle$. From (15) one finds that their stationary values are determined by the noise amplitudes, as well as the parameters ϵ and b : $C_{xx}^0 = -\frac{D_1+D_2}{1-b^2}$, $C_{yy}^0 = -D_2(1-b^2) - \epsilon\frac{D_1+D_2}{1-b^2}$ and $C_{xy}^0 = -D_2$. The system (15) can be linearized about these stationary values, considering the perturbations of the form $K_{xx} = C_{xx}(t, t') - C_{xx}^0 = Ae^{i\lambda t}$, $K_{yy} = C_{yy}(t, t') - C_{yy}^0 = Be^{i\lambda t}$ and $K_{xy} = C_{xy}(t, t') - C_{xy}^0 = Ce^{i\lambda t}$. For fixed $b = 1.05$ and $\epsilon = 0.01$, the ensuing characteristic equation $2\epsilon^2\lambda^3 - 3\epsilon\lambda^2(1-b^2) + \lambda(1-b^2)^2 - (1-b^2)e^{-\lambda\tau_{in}} = 0$ indicates that the stability of the stationary solution depends solely on τ_{in} . It may be shown numerically that the critical value of τ_{in} for the second moments is virtually indistinguishable from the critical threshold τ_{in}^H obtained for the first moments.

3.3. Method of statistical linearization

As a means of characterizing the co-effects of noise and τ_{in} on the behavior of a single unit, we invoke an approach that belongs to a corpus of statistical linearization techniques [40,39]. Such methods have originally been developed to gain insight into the interplay of noise and nonlinearity in stochastically perturbed systems. The general idea is to substitute the nonlinear terms with their stationary values calculated in the self-consistent fashion, whereby the impact of noise on the system's dynamics is ultimately reduced to a dependence on the noise amplitude. Note that the latter property is reminiscent to what is typically obtained by the mean-field approaches [41–45].

The immediate goal is to translate the original dynamics of a single unit into an analogous two-dimensional Ornstein–Uhlenbeck process, described by a system of linear SDEs of the form [46]

$$d\mathbf{x}_s(t) = -\hat{A}\mathbf{x}_s(t)dt + \hat{B}d\mathbf{W}(t),\tag{16}$$

where bold letters indicate vectors, \hat{A} and \hat{B} are the appropriate two-dimensional matrices, and the index s refers to the stationary process with a zero mean. Principal gain from the transformation is related to the point that the result for the stationary variance matrix $\hat{\sigma}$ of an Ornstein–Uhlenbeck process in two dimensions is well known and can be applied to calculate the second moments of the fast and slow variables. In order to proceed, one is required to introduce two approximations: (i) τ_{in} is small so that the expansion of the term containing delay $y(t - \tau_{in}) \approx y(t) - \tau_{in}\frac{dy}{dt}$ to the first order is sufficient, and (ii) the nonlinear term $x^3(t)$ is replaced by $x^3(t) \approx \langle x^2 \rangle_t x(t)$, where the t index on angled brackets denotes a stationary, i.e. time-averaged quantity.

As an example, we consider the scenario with external noise, which is also preferred given the approximation (i). Moving to a new set of coordinates shifted for the position of the equilibrium (x_0, y_0) and having implemented (i) and (ii), one finds that

$$\hat{A} = \begin{pmatrix} -\mu/\epsilon & 1/\epsilon \\ -1 & 0 \end{pmatrix}, \quad \hat{B} = \begin{pmatrix} \sqrt{2D_1/\epsilon} & 0 \\ 0 & 0 \end{pmatrix}, \quad \mathbf{x}_s = \begin{pmatrix} x \\ y \end{pmatrix},\tag{17}$$

with $\mu = 1 - b^2 + \tau_{in} - \frac{1}{3}\langle x^2 \rangle_t$. $\langle x^2 \rangle_t$ may be calculated in a self-consistent fashion by using the expression for the stationary variance matrix of a two-dimensional Ornstein–Uhlenbeck process [46]

$$\hat{\sigma} = \frac{(\text{Det}\hat{A})\hat{B}\hat{B}^T + [\hat{A} - \text{Tr}\hat{A}\hat{I}]\hat{B}\hat{B}^T[\hat{A} - \text{Tr}\hat{A}\hat{I}]^T}{2\text{Tr}\hat{A}\text{Det}\hat{A}}, \tag{18}$$

where the superscript T refers to a transposed matrix and \hat{I} denotes the identity matrix. In particular, one can demonstrate that from (18) follows

$$\hat{\sigma}_{11} = \langle x^2 \rangle_t = -D_1/\mu = -D_1 / \left[1 - b^2 + \tau_{in} - \frac{1}{3} \langle x^2 \rangle_t \right], \tag{19}$$

which presents a second order equation over $\langle x^2 \rangle_t$. Given that the solution has to be positive, we finally obtain

$$\langle x^2 \rangle_t = \frac{1}{2} \left[3(1 - b^2 + \tau_{in}) + \sqrt{12D_1 + 3(1 - b^2 + \tau_{in})^2} \right]. \tag{20}$$

Inserting this result into the above expression for μ , it is easy to show that $\mu < 1 - b^2 + \tau_{in}$ holds for any D_1 and reasonably small τ_{in} under $b = 1.05$, the value kept throughout the paper. This is important because the stability of the equilibrium for the linearized system given by (17) is determined by the characteristic roots $\lambda_{\pm} = \frac{\mu \pm \sqrt{\mu^2 - 4\epsilon}}{2\epsilon}$, where μ plays a key role. What the above point actually means is that the net effect of external noise, contributing via the $\langle x^2 \rangle_t$ term, is to drive the system away from the critical threshold of the Hopf bifurcation controlled by b . In other words, presence of D_1 makes the unit “less” excitable, which is the same type of influence already attributed to τ_{in} .

Nevertheless, our main result obtained by the method of statistical linearization concerns the interplay of external noise and τ_{in} . To assess how these ingredients affect the unit’s oscillatory behavior, one may consider the dependence of correlation time t_{corr} as a function of D_1 and τ_{in} . The latter provides a useful measure for regularity of oscillations, and may indicate how the competition between the noise- and the delay-driven mode is resolved for the given parameter set. Note that the correlation time [29,39] is defined by

$$t_{corr} = \int_0^\infty |G_{xx}(s)| ds, \tag{21}$$

where $G_{xx}(s)$ stands for the normalized autocorrelation function $G_{xx}(s) = \frac{1}{\sigma_x^2} \langle x(t-s)x(t) \rangle_t$, knowing that $\langle x \rangle_t = 0$. In general, the expression for the time correlation matrix of a multivariate stationary Ornstein–Uhlenbeck process reads [46]

$$\hat{G}(s) = \langle \mathbf{x}(t-s), \mathbf{x}^T(t) \rangle_t = \hat{\sigma} \exp[-\hat{A}^T s], \tag{22}$$

which may be applied to calculate t_{corr} from (21).

Skipping the more involved details of the calculation, here we just report on the results, given in Fig. 3 in terms of the family of curves $t_{corr}(D_1)$ for a set of relevant τ_{in} values $\tau_{in} \in \{0, 0.1, 0.2, 0.4\}$. One first learns that the applied method provides accurate qualitative predictions regarding the effects of τ_{in} : for $\tau_{in} = \{0, 0.1\}$ there is no delay-driven mode, so the corresponding curves lie below the ones for $\tau_{in} = \{0.2, 0.4\}$ within the entire range of D_1 values. Also, for larger D_1 , all the curves approach each other, indicating that the delay-led behavior is completely overwhelmed by noise. The values of t_{corr} for $\tau_{in} = \{0.2, 0.4\}$ are very large only for small $D_1 \sim 10^{-4}$ and decay rapidly with increasing noise. The point that t_{corr} is three orders of magnitude smaller at intermediate noise $D_1 \sim 10^{-3}$ than at $D_1 \sim 10^{-4}$ but is still above the curves for $\tau_{in} = \{0, 0.1\}$ implies that some form of coherent motion exists, but is not prevalingly deterministic, i.e. it is not driven by the delay. This is consistent with the numerical findings on the average ISIs, e.g. at $\tau_{in} = 0.4$, the average ISI for $D_1 = 0.002$, $\langle T \rangle = 2.52$, is substantially distinct from $\langle T \rangle = 4.29$ obtained for $D_1 = 0.0001$.

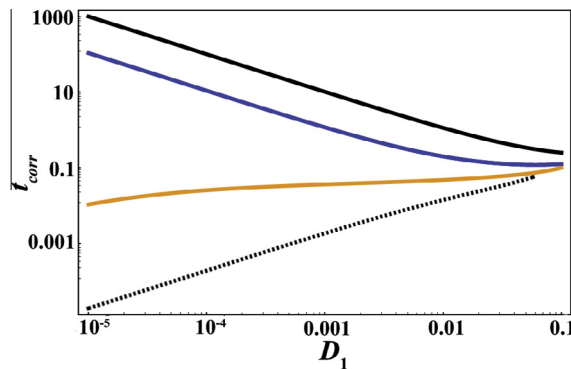


Fig. 3. Variation of correlation time t_{corr} with external noise D_1 for a single unit, as obtained by the method of statistical linearization. The curves from bottom to top correspond to $\tau_{in} = 0, 0.1, 0.2$ and 0.4 , respectively.

4. Stability analysis for the system of interacting units

Having considered the issues related to stability of an single unit in presence of noise and τ_{in} , here we address the analogous problem for the system of two interacting FHN excitable elements, which involves coupling delay τ_{ex} as an additional ingredient. For the most part, the analysis is focussed on the deterministic version of (1) with $c > 0, D_1 = D_2 = 0$. This approach is taken for two reasons: (i) due to interplay of τ_{in} and τ_{ex} , the deterministic system alone displays intricate behavior, including bistable regimes between the different oscillatory modes in multiple parameter domains, and (ii), conditions for stability of the unperturbed system coincide with those for the first moments of the linearized system influenced by noise. Naturally, the bifurcation analysis to follow will provide a useful tool for interpretation of the numerically obtained results on the competition between the noise- and the delay-driven modes, serving as the reference point to clearly isolate the stochastic effects.

The characteristic equation describing local stability of equilibrium $(x_i, y_i) = (-b, -b + b^3/3), i \in \{1, 2\}$ for the deterministic version of system (1) reads

$$\lambda^2 [\epsilon\lambda - (1 - b^2 - c)]^2 + 2\lambda [\epsilon\lambda - (1 - b^2 - c)] e^{-\lambda\tau_{in}} - \lambda^2 c^2 e^{-2\lambda\tau_{ex}} - e^{-2\lambda\tau_{in}} = 0. \quad (23)$$

Given the complexity of the above expression, local stability analysis has been carried out numerically by the *DDE – biftool* [47,48], an adaptable package of *MATLAB* routines suitable for handling the sets of DDE with constant delays. The issue of particular interest is how the behavior of coupled units is influenced by variation of τ_{in} and τ_{ex} while c is kept fixed. It turns out that the system undergoes a sequence of supercritical and subcritical Hopf bifurcations, whereby the former (latter) result in creation of a stable (unstable) limit cycle. Recall that both types of Hopf bifurcation can further be cast as direct or inverse [49], which indicates whether an unstable two-dimensional manifold for the fixed point appears or vanishes when crossing the bifurcation curve, causing the fixed point to unfold on the unstable or the stable side, respectively. In the following, we use the notation where the $+/-$ sign reflects the direct/inverse character of bifurcation, whereas the numerical indices refer to the order in which the successive branches of bifurcation curves are encountered as τ_{ex} is increased.

Bifurcation diagram in the $\tau_{ex} - \tau_{in}$ parameter plane for the moderate coupling strength $c = 0.1$ is shown in Fig. 4. We stress that the complete knowledge on the system's behavior cannot be gained by performing the local bifurcation analysis alone, since τ_{ex} and τ_{in} each give rise to a global fold-cycle bifurcation as well. Due to global character of such events, the fashion in which the observed dynamics is shaped may be interpreted as if the effects of coupling were just superimposed on the behavior governed by the intrinsic properties of units, which results in multistable regimes for most of the relevant parameter domains. Focussing first on the case $\tau_{ex} = 0$, we note that the scenario for the onset of oscillations exactly matches the one that holds for an isolated unit. In brief, under increasing τ_{in} , the system first undergoes fold-cycle bifurcation at $\tau_{in}^{FC} = 0.106$, see the point denoted by an open circle in Fig. 4, and then displays a subtle interplay between the local Hopf and the global bifurcation around $\tau_{in}^0 = 0.118$. The latter rests on the fact that the incipient cycle emerging from the Hopf bifurcation lies enclosed by the saddle-cycle left over from the global bifurcation, which for some weakly supercritical τ_{in} leads to their collision and disappearance following an inverse fold-cycle bifurcation. Consequently, after a small interval of bistability, the system's unique attractor for $\tau_{ex} = 0$ and $\tau_{in} \gg \tau_{in}^0$ is the large cycle, whose existence is unaffected by the local bifurcations.

On the other hand, for $\tau_{in} = 0$, one finds that a fold-cycle bifurcation controlled by τ_{ex} occurs around $\tau_{ex}^{FC} = 1.16$, cf. the black circle in Fig. 4. Therefore, in terms of stability, the system lies in the stationary state for $\tau_{ex} < \tau_{ex}^{FC}, \tau_{in} < \tau_{in}^{FC}$, whereas the domain $\tau_{ex} \geq \tau_{ex}^{FC}, \tau_{in} < \tau_{in}^{FC}$ is characterized by a coexistence between the fixed point and a limit cycle, whose basins of attraction are separated by the saddle-cycle created in the global bifurcation. Note that the large cycles emerging from the global bifurcations evoked by τ_{ex} or τ_{in} have very distinct phase portraits, cf. Fig. 2. The orbit of the former mostly follows

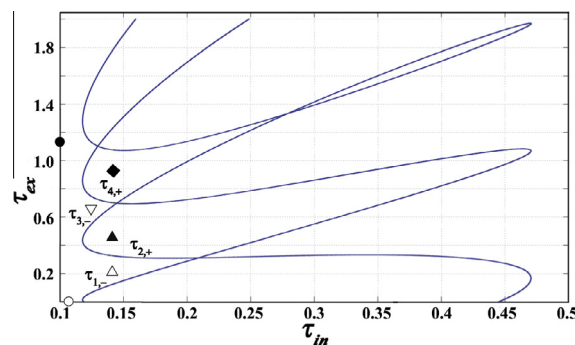


Fig. 4. Bifurcation diagram $\tau_{ex} - \tau_{in}$ for the two interacting units in the noiseless case. Stability of equilibrium is influenced by a sequence of direct and inverse supercritical and subcritical Hopf bifurcations. Critical values for the global fold-cycle bifurcations are indicated by an open and solid circle. Coupling strength is set to $c = 0.1$.

the cubic nullcline, whereas the latter one's traverses a large section away from the nullcline. Furthermore, the period associated with oscillations at $\tau_{ex}^{FC}, T_* = 2.42$, is significantly smaller than $T_\circ = 3.96$.

Let us now turn to the sequence of local bifurcations occurring under increasing τ_{ex} for $\tau_{in} \gtrsim \tau_{in}^0$. In the domain indicated by an open up-triangle in Fig. 4, stability of equilibrium is regained as a result of an inverse subcritical Hopf bifurcation which the system undergoes at $\tau_{1,-}$. This means that the region $\tau_{1,-} < \tau_{ex} < \tau_{2,+}$ admits a bistable regime where the large cycle and the stationary state coexist. Note that the unstable cycle born in the Hopf bifurcation acts like a threshold switching between the two stable solutions. Stepping into the area marked by a solid up-triangle in Fig. 5, the equilibrium becomes unstable due to a direct supercritical Hopf bifurcation at $\tau_{2,+}$. However, one finds that another bistable regime is established, which involves coexistence between two limit cycles, a large one created in the fold-cycle bifurcation and the other emerging from the Hopf bifurcation. Crossing the curve $\tau_{3,-}$ from below, cf. the domain marked by an open down-triangle in Fig. 5, the fixed point loses an unstable plane due to an inverse subcritical Hopf bifurcation, thus becoming stable again. In the region bounded by $\tau_{3,-}$ and $\tau_{4,+}$, bistability between two oscillatory states is replaced by a regime where the stationary state coexists with an oscillatory solution. Above $\tau_{4,+}$, the most important point is that the equilibrium is no longer stable for any τ_{ex} . Apart from the direct supercritical Hopf bifurcation which the system undergoes at $\tau_{4,+}$, this is further linked with the fact that the increase of τ_{ex} gives rise to a global fold-cycle bifurcation, as explained earlier. Just below τ_{ex}^{FC} , it is difficult to discern between the modes arising from the local bifurcation and the global bifurcation induced by τ_{in} , with the associated periods becoming barely distinguishable. Above τ_{ex}^{FC} , one could in principle expect a multistable regime characterized by three oscillations modes, one elicited by the local, and the remaining two by the global events. Nevertheless, it turns out that the structure of phase space may support only two coexisting oscillatory states. Apparently, the limit cycle born via Hopf bifurcation vanishes by a scenario involving an inverse fold-cycle bifurcation, where it collides with one of the saddle cycles.

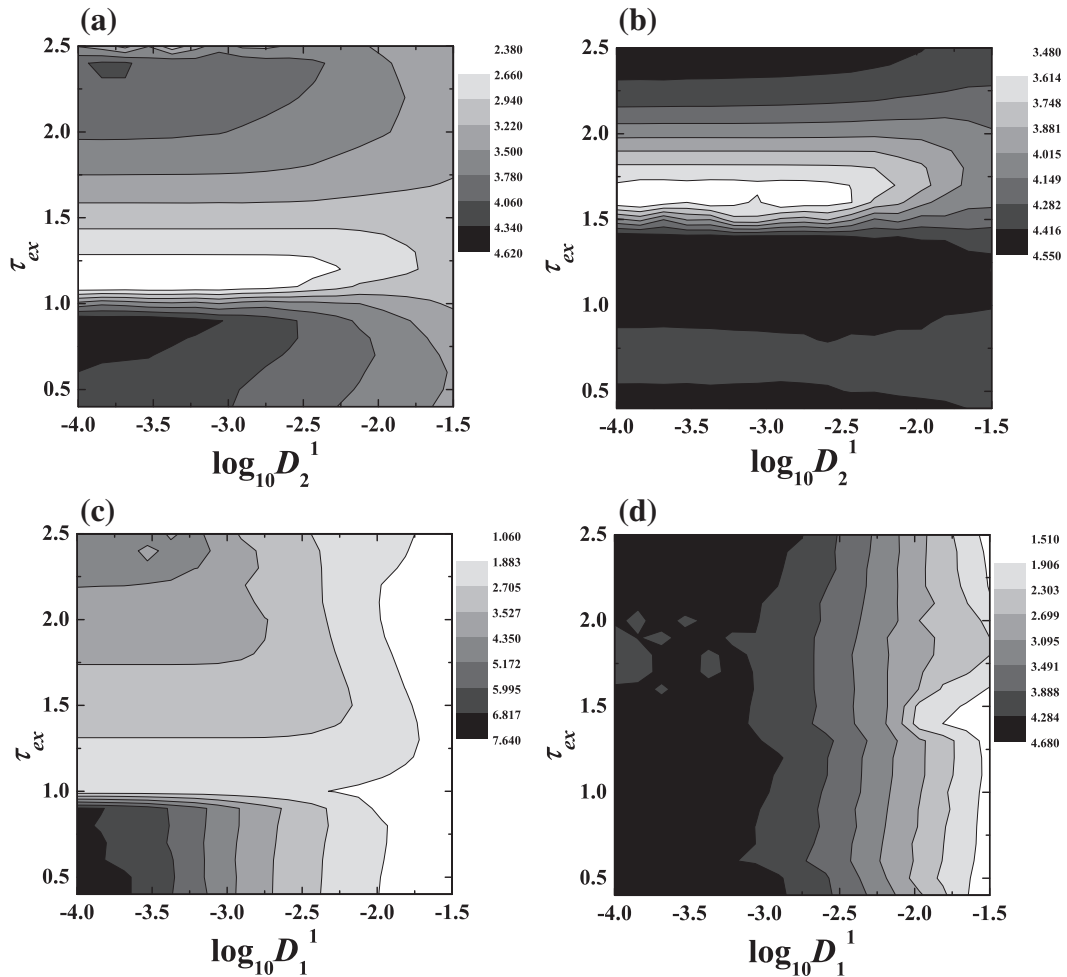


Fig. 5. Indication on competition between the noise-induced and delay-driven modes. Average ISIs (T_1) for the adjustable unit are plotted as a function of its noise intensity and τ_{ex} . The top row refers to setup with internal, and the bottom row with external noise. The left and right columns show the fields obtained for $\tau_{in} = 0$ and $\tau_{in} = 0.4$, respectively.

As a result, a bistable regime is established, such that the two large cycles from the global bifurcations coexist, with the corresponding attraction basins separated by the remaining saddle cycle. For $\tau_{in} \gtrsim \tau_{in}^0$, the given oscillation modes have clearly distinct periods.

Detailed analysis on the deterministic system has mostly been motivated by its specific feature that the dynamics is substantially influenced by the global, rather than local bifurcations. A question that naturally arises is how is this point reflected in the stability of the system influenced by noise. As explained in case of an isolated unit, conditions for the stability of the deterministic system exactly match those associated with the first moments of the perturbed system. The dynamics of second moments is given by a complex set of equations, which are best treated numerically. However, judging by the above findings, even the complete knowledge on the stability of the linearized system would be insufficient to fully understand the behavior displayed by the interacting units under stochastic perturbation. On the other hand, note that the results obtained for the deterministic system also hold for the perturbed system in the limit of small noise, though some of the bistable regimes, especially those involving the equilibrium, are likely to be highly sensitive to stochastic effects. Apart from disturbing the stability of equilibrium, stronger noise may affect the attraction basins of coexisting attractors thereby modifying the asymptotic dynamics, or can give rise to certain transient phenomena, such as mixing between the different oscillatory modes. Analysis on these issues, as well as coherence and synchronization properties of interacting units under a wide range of noise amplitudes has been performed by numerical means.

5. Numerical results on the interplay of noise and the delays

In this section, the goal is to demonstrate how is the competition between the delay- and noise-driven modes reflected in the coherence of individual firing series and the units' synchronization. Since oscillatory motion is either induced or perturbed by noise, a quantity appropriate to characterize the degree of coherence over a long series $x_i(t)$ is the ratio of the time-averaged ISI and the standard deviation of the ISI distribution [50]

$$S_i = \frac{\langle T_{i,k} \rangle_t}{\sqrt{\langle T_{i,k}^2 \rangle_t - \langle T_{i,k} \rangle_t^2}}. \quad (24)$$

In (24), i specifies the particular unit, $T_{i,k} = t_{i,k+1} - t_{i,k}$ refers to the k th interspike interval, and the spike time $t_{i,k}$ is defined as the moment of crossing the threshold $x_i(t) = 1$ under condition $x_i'(t_k) > 0$. Note that S_i , often referred to as regularity, may be interpreted as a signal-to-noise ratio [25], in a sense that it compares the recorded noisy signal to a periodic one, whose $P(T_{i,k})$ distribution would conform to a delta-function. In neuroscience, quantity S_i is deemed relevant because it can be linked to the timing precision of information processing [51].

Given the noisy nature of oscillations, coordinated activity between the units is considered within the framework of stochastic synchronization. This concept comprises frequency synchronization, where the time-scales characterizing oscillatory motion of the involved systems are adjusted, or phase synchronization, which refers to scenario where an approximately constant phase difference between the units is maintained. On the former, note that the appropriate time-scale for each unit is associated with the average ISI, whose reciprocal value can be viewed as the firing frequency. Therefore, as a measure of frequency synchronization one may use the ratio of time-averaged ISIs, $r = \langle T_{1,k} \rangle_t / \langle T_{2,k} \rangle_t$ [29]. The case of special interest concerns frequency entrainment between the units where $r \approx 1$. We stress that the latter condition does not imply per se that the oscillatory motions of the two units take place on the same attractor. In particular, r merely refers to adjustment of time-scales between oscillatory motions regardless of their specific features, such as the oscillation amplitudes or phases.

To examine coordination of units' spiking at an arbitrary moment of time, we define the phase [52,53]

$$\phi_i(t) = 2\pi \frac{t - t_{i,k-1}}{t_{i,k} - t_{i,k-1}} + 2\pi(k - 1), \quad (25)$$

where the notation is analogous to that in (24). For systems comprised of coupled autonomous oscillators, phase synchronization, or rather phase locking, would imply that the phase difference $\Delta\phi(t) = \phi_1(t) - \phi_2(t)$ remains constant during the evolution. In presence of noise, $\Delta\phi(t)$ cannot maintain a stationary value, but its fluctuations may appear nearly stationary for most of the time if perturbation is weak. Nevertheless, even then the abrupt jumps are bound to occur due to phase slips [29,53], where $\Delta\phi(t)$ changes by $\pm 2\pi$. Consequently, better phase synchronization between the units effectively implies that the intervals with nearly constant relative phase last longer. The degree of phase synchronization is quantified by the synchronization index γ [53,29]

$$\gamma = \sqrt{\langle \cos \Delta\phi(t) \rangle_t^2 + \langle \sin \Delta\phi(t) \rangle_t^2}, \quad (26)$$

which can vary within $\gamma \in [0, 1]$ interval, such that values approaching 1 describe approximate phase synchronization. Note that γ by construction refers only to adjustment of phases between the oscillating units, independent on the potentially different oscillation amplitudes [53]. This is convenient, because we encounter instances where the two units lie on distinct limit cycles, but the associated characteristic time-scales are closely matched.

The strategy adopted to systematically examine the co-effects of noise, τ_{ex} and τ_{in} on behavior of two interacting excitable units is as follows. We distinguish between two basic setups, characterized by whether perturbation derives from external or

internal sources. In both instances, action of noise is analyzed by having an “adjustable” unit (index $i = 1$) with variable noise amplitude D_1^1 or D_1^2 , and a unit that is “optimized” ($i = 2$) in a sense that D_2^1 or D_2^2 are kept at the appropriate resonant value, be it the CR or the SISR case. Coupling delay spans the interval $\tau_{ex} \in [0.4, 2.5]$, selected such that the lowest value is an order of magnitude less than the typical ISI, whereas the highest value is comparable to it. Coupling strength is fixed to an intermediate value $c = 0.1$, which is sufficient to facilitate coordinated activity between the units, rather than let their dynamics remain independent. Qualitative impact of intrinsic delay is outlined by comparing the system’s behavior for domains where τ_{in} lies below or above τ_{in}^{FC} , having them represented by $\tau_{in} = 0$ and $\tau_{in} = 0.4$, respectively.

In the discussion below, the aim is to numerically demonstrate four points, conditionally divided into primarily stochastic and primarily deterministic effects. Regarding the first group, one finds that the distinction between external/internal character of noise crucially influences (i) the ability of entrainment to a single frequency and (ii) the fashion in which the competition between the delay- and noise-driven modes is resolved. As for the second group, τ_{in} is established to substantially influence (i) regularity of firing and (ii) the properties of phase synchronization between the units. Note that the dependencies of S_i and γ on D_1^1 or D_1^2 and the delays are obtained by performing time-averages over long $x_i(t)$ series, as well as the stochastic averages over an ensemble of $\sim 10^2$ realizations, making certain that the transients have been eliminated and that further increasing of the ensemble size does not significantly affect the results stated. Numerical integration has been carried out by the Euler integration scheme with time step 0.001. We have adopted the standard and physically plausible initial functions, based on the assumption that the units evolve independently within the time interval $t \in [-\tau_{min}, 0]$, where $\tau_{min} = \min\{\tau_{in}, \tau_{ex}\}$. In effect, for the specified interval, the system (1) has been integrated by setting aside the interaction terms, with the initial conditions lying in close vicinity of equilibrium.

5.1. Frequency synchronization and the competition between the delay-driven and noise-induced modes

Regarding frequency entrainment, a qualitatively different picture emerges for the setups involving external or internal noise. In the latter case, one finds that the units exhibit frequency synchronization within all the considered parameter domains. This has been verified by determining that $r \approx 1$ holds for all the plausible values of τ_{in} under variation of τ_{ex} and D_1^2 . On the other hand, under external noise, for $\tau_{in} = 0$ or any relevant $\tau_{in} > 0$, frequency synchronization is gradually lost with D_1^1 , whereby the decline of r becomes marginally steeper at higher τ_{in} . In other words, frequency entrainment is more sensitive to external than the internal perturbation. Note that by increasing external noise at adjustable unit, its average firing frequency is enhanced, but it fails to control the optimized unit, so the two eventually act as if they were independent. Naturally, existence of a prevailing mode in the system’s behavior can only be considered if there is frequency entrainment.

The point on the prevailing oscillatory modes is best illustrated by examining variation of the average ISIs in the $\tau_{ex} - D_2^1$ ($\tau_{ex} - D_1^1$) plane for internal (external) noise. In Fig. 5, and Fig. 5(b) are shown the fields $\langle T_1 \rangle(\tau_{ex}, D_2^1)$ referring to the cases $\tau_{in} = 0$ and $\tau_{in} = 0.4$, respectively. Given the frequency synchronization, nearly identical results would be obtained by plotting $\langle T_2 \rangle(\tau_{ex}, D_2^2)$ instead. For $\tau_{in} = 0$, one learns that three qualitatively distinct regimes are clearly discernible under increasing τ_{ex} , which may be explained by invoking the arguments from Section 4. In the domain below the fold-cycle bifurcation ($\tau_{ex} \lesssim \tau_{ex}^{FC}$), the adjustable unit is able to entrain the optimized one, which is corroborated by the fact that the average ISI strongly depends on D_2^2 . Once the global bifurcation has occurred ($\tau_{ex}^{FC} \approx 1.16$), there is an interval of τ_{ex} values where the units’ oscillatory motion is dominated by the coupling delay. This point is verified by the rather weak dependence of $\langle T_1 \rangle$ on D_2^1 . Note that the characteristic time-scale of oscillations in this region is described by an approximate relation $\langle T_1 \rangle \approx 2\tau_{ex}$.

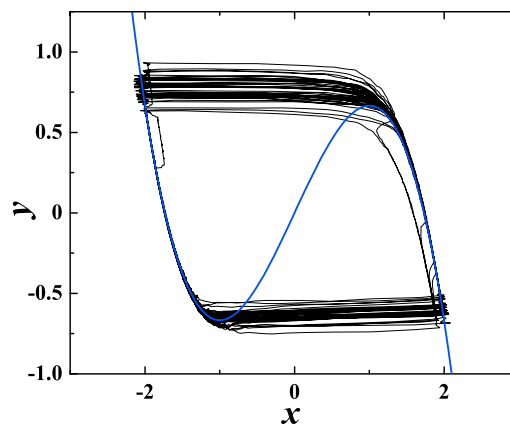


Fig. 6. Noise may induce stochastic switching between different oscillatory modes. The phase portrait corresponds to the adjustable unit under internal noise, with the parameters set to $D_2^1 = 0.001$, $D_2^2 = 0.00255$, $\tau_{ex} = 1.7$, $\tau_{in} = 0$. In the particular instance, noise causes mixing between the mode driven by τ_{ex} and the noise-induced mode derived from the optimized unit. The cubic nullcline is drawn to indicate the distinction between the two types of orbits more clearly.

Entrainment with coupling delay is gradually lost as τ_{ex} further departs from τ_{ex}^{FC} . Before the third regime actually sets in, one encounters an interval of coupling delays ($\tau_{ex} \approx 1.7$), where the distributions of ISIs $P(T_{i,k})$ are not unimodal even for very small D_2^1 . In particular, a typical $P(T_{i,k})$ for long $x_i(t)$ series in this τ_{ex} range indicates strong mixing between the τ_{ex} -driven mode and the noise-induced mode of the optimized unit, whereby the latter component eventually prevails. Stochastic switching between the limit cycles characterizing the two modes is illustrated in Fig. 6. Note that despite the mixing, in statistical sense the units display the same average behavior, such that the ratio $r \approx 1$ is maintained. The delays $\tau_{ex} \geq 1.9$ admit the regime where, at variance with the case $\tau_{ex} \lesssim \tau_{ex}^{FC}$, the optimized unit is able to entrain the adjustable one. Naturally, such form of motion is likely to be susceptible to noise if $D_2^1 > D_2^2$, which is confirmed by the shape of the field $\langle T_1 \rangle(\tau_{ex}, D_2^1)$, cf. Fig. 5(a).

The picture described so far is substantially modified by the non-trivial $\tau_{in} > \tau_{in}^{FC}$, see Fig. 5(b). For this setup, there are two qualitatively different regimes, but the one where the characteristic time-scales of both units are controlled by τ_{in} prevails for most of the (τ_{ex}, D_2^1) parameter values. It is interesting that the coupling term is able to suppress such a behavior only for $\tau_{ex} \in (1.6, 1.9)$. Within this interval, the characteristic time-scale for the τ_{ex} -driven mode approximately matches the one for the noise-driven mode at the optimized unit. Above $\tau_{ex} \approx 1.9$, the mode owing to τ_{in} wins over again, such that the units display longer average ISIs, cf. Fig. 5(b).

Now let us turn to the scenario involving external noise. Given the loss of frequency synchronization for larger D_1^1 , the average dynamics of units 1 and 2 is governed independently. In Fig. 5(b) and (d) we have plotted the fields $\langle T_1 \rangle(\tau_{ex}, D_1^1)$ corresponding to $\tau_{in} = 0$ and $\tau_{in} = 0.4$, respectively. The behavior of unit 1 is illustrated rather than that of unit 2, because it is more strongly affected by the change from internal to external noise. Note that below τ_{in}^{FC} , the prevailing dynamics of the optimized unit conforms to the paradigm involving three characteristic regimes, similar to what is shown in Fig. 5(a). As for the adjustable unit, once D_1^1 becomes sufficiently strong ($D_1^1 \gg D_2^1$), it completely overwhelms all the other influences, implying that the unit 1 can no longer be entrained either by τ_{ex} or the optimized unit. This is reflected by the virtual independence of $\langle T_1 \rangle$ on τ_{ex} for larger D_1^1 , cf. Fig. 5(c). For τ_{in} above τ_{in}^{FC} , it turns out that the effects of coupling are felt even less than for the

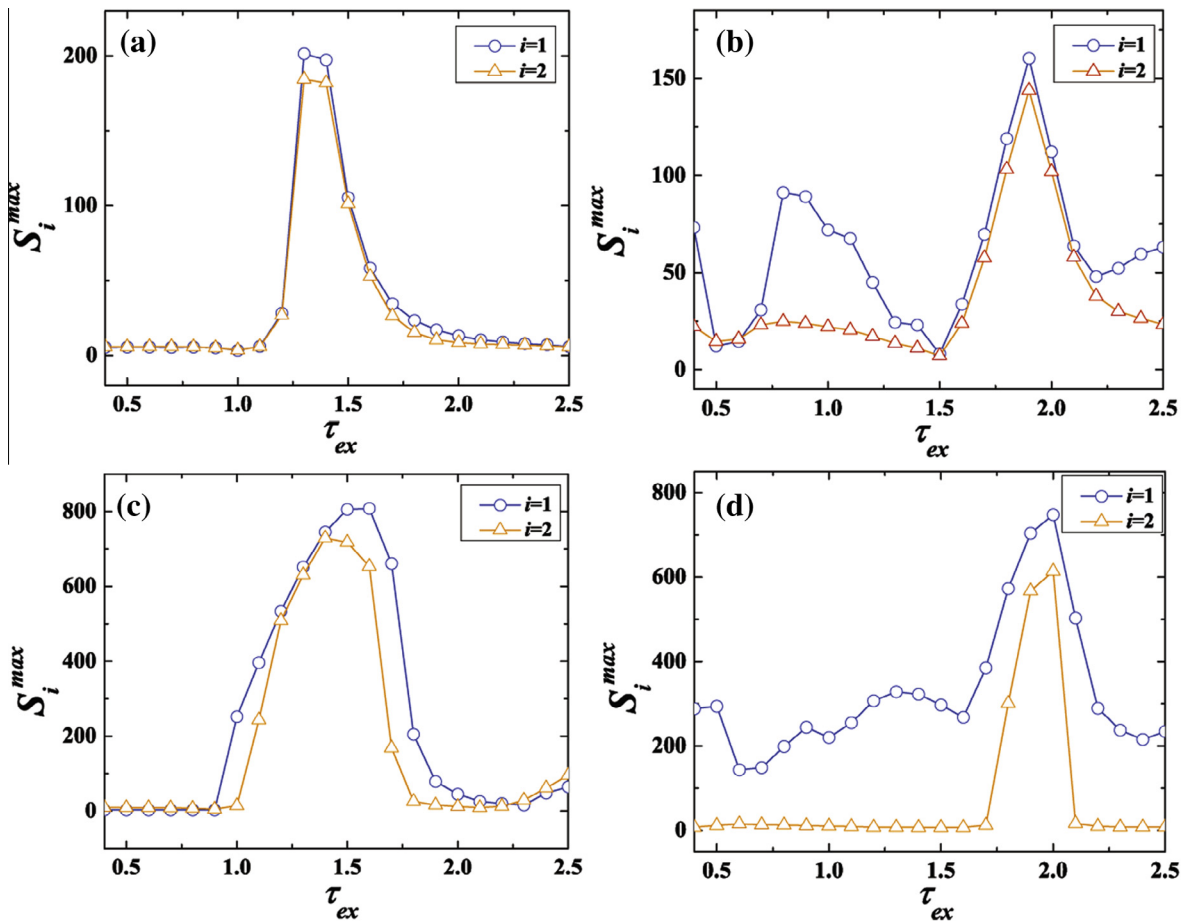


Fig. 7. Families of curves $S_i^{max}(\tau_{ex})$, whereby open circles (triangles) refer to unit $i = 1$ ($i = 2$). The presentation scheme is such that the top and bottom rows concern the scenarios with internal and external noise, respectively, whereas the left column illustrates the case $\tau_{in} = 0$, and the right one the case $\tau_{in} = 0.4$. The profile of curves suggests that firing coherence is substantially influenced by τ_{in} .

analogous scenario with internal noise. This may be attributed to the point that the coupling term itself attains a noisy component, at variance with the previous setup. While the dynamics of unit 2 is completely controlled by τ_{in} , the data in Fig. 5(d) demonstrate that unit 1 exhibits a τ_{in} -driven mode only for smaller D_1^1 , approximately given by the condition $D_1^1 < D_2^1$. In line with the results derived in subSection 3.3, for larger D_1^1 the characteristic time-scale of oscillations at unit 1 is set by noise. This is corroborated by the fact that $\langle T_1 \rangle$ strongly changes with D_1^1 , but remains unaffected by the increase of τ_{ex} , see Fig. 5(d).

5.2. Regularity of firing and phase synchronization

In order to isolate the key ingredients influencing regularity, one first performs a kind of coarse-graining over the effects of noise. The latter consists in determining $S_i^{max}(\tau_{ex}, \tau_{in})$, which present the largest values of signal-to-noise ratio over the considered range of noise amplitudes (D_1^1 or D_2^1) acting on unit 1 under the fixed pair of delays (τ_{ex}, τ_{in}) . In Fig. 7 are illustrated the dependencies $S_i^{max}(\tau_{ex})$ for external (top row) and internal noise (bottom row), whereas the left and right columns refer to cases $\tau_{in} = 0$ and $\tau_{in} = 0.4$, respectively. At first sight, it becomes apparent that the prevailing behavior is determined by the intrinsic delay, while variation with the type of noise is only a secondary effect. For τ_{in} below τ_{in}^{FC} , the peak in $S_i^{max}(\tau_{ex})$ reflects the onset of the fold-cycle bifurcation controlled by τ_{ex} . Nevertheless, the peak's profile and the position of its maximum relative to τ_{ex}^{FC} is influenced by the form of noise. In particular, it seems likely that the peak's maximum coincides with the τ_{ex} value where the noise-induced oscillations at unit 2 provide the weakest perturbation to the τ_{ex} -driven mode.

For intrinsic delays above τ_{in}^{FC} , both $S_1^{max}(\tau_{ex})$ and $S_2^{max}(\tau_{ex})$ exhibit a sharp peak around $\tau_{ex} \approx 2$. Nonetheless, motion of the adjustable unit is further characterized by the secondary peak or peaks, contingent on the external/internal character of noise. Note that Fig. 7 refers only to coupling delays that satisfy $\tau_{ex} > \tau_{in}$, so the regularity peak corresponding to oscillations induced by the τ_{in} -controlled global bifurcation is not visible. The primary peak itself in Fig. 7(c) and (d) can be linked to scenario where the characteristic time-scales of the τ_{ex} -induced mode and the noise-driven mode at the optimized unit are most closely matched, such that the stochastic effects are minimized. On the other hand, increase of S_1^{max} at smaller τ_{ex} values actually reflects the adjustable unit's motion for very small D_1^1 or D_2^1 , which warrant that the τ_{in} -driven mode is perturbed the least.

The latter point suggests one should examine in greater detail how much the maximal regularities represent the general tendencies in system's behavior, taking into account both the character of noise and its magnitude. It turns out that the above description is more accurate if the perturbation is due to internal, than the external sources. In the latter instance, the provided picture is valid only for small D_1^1 , where the frequency synchronization is still maintained. In this context, one should also make it explicit how the coaction of non-trivial $\tau_{in} > \tau_{in}^{FC}$ and noise affects S_i at specific τ_{ex} values. For τ_{ex} below τ_{ex}^{FC} , it is readily seen that the deterministic component emerging due to $\tau_{in} > \tau_{in}^{FC}$ improves the firing coherence of both units compared to what is found at $\tau_{in} < \tau_{in}^{FC}$. Such a behavior is illustrated in Fig. 8(a) showing families of curves $S_i(D_2^1)$ for $\tau_{in} = 0$ and $\tau_{in} = 0.4$ at fixed $\tau_{ex} = 0.8$. On the other hand, for $\tau_{ex} > \tau_{ex}^{FC}$ the stochastic effects come into play more strongly. In the domain $\tau_{ex} \in (1.2, 1.9)$, the intrinsic delay above τ_{in}^{FC} may promote or suppress regularity for small noise, depending on whether it derives from external or internal sources. Under larger perturbation, regularity tends to decrease due to stochastic switching between the two deterministic modes, one driven by τ_{ex} , and the other by τ_{in} . An example where setting intrinsic delay above τ_{in}^{FC} is accompanied by the nontrivial dependence of S_i on noise is illustrated in Fig. 8(b), which shows how S_i vary with D_2^1 for $\tau_{in} = 0$ and $\tau_{in} = 0.4$ at fixed $\tau_{ex} = 1.7$.

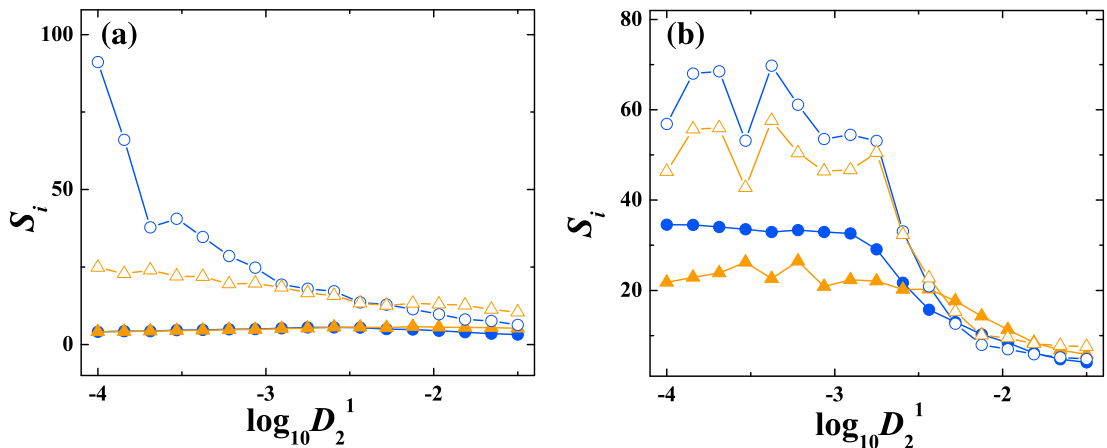


Fig. 8. Whether and how much setting τ_{in} above τ_{in}^{FC} contributes to spiking coherence depends nontrivially on τ_{ex} and noise at unit 1. (a) and (b) show $S_i(D_2^1)$ families of curves for $\tau_{in} = 0$ (solid symbols) and $\tau_{in} = 0.4$ (open symbols), obtained under fixed $\tau_{ex} = 0.8$ and $\tau_{ex} = 1.7$, respectively. The circles (triangles) are reserved for unit 1 (2). The data in both instances refer to setup including internal noise with $D_2^2 = 0.00255$.

As announced at the beginning of this section, we address the issue of phase synchronization by considering variation of the synchronization index γ . Adhering to the scheme of analysis so far, in Fig. 9 are illustrated the dependencies $\gamma(\tau_{ex}, D_2^1)$ (top row) and $\gamma(\tau_{ex}, D_1^1)$ (bottom row) obtained for internal and external sources of noise, whereas the left and right columns refer to cases $\tau_{in} = 0$ and $\tau_{in} = 0.4$, respectively. In the insets are shown the auxiliary plots $\gamma^{max}(\tau_{ex})$, intended to help in identifying the domains supporting phase synchronization. Note that γ^{max} follow from the same coarse-graining procedure as S_1^{max} introduced earlier on.

For τ_{in} below τ_{in}^{FC} , one finds three τ_{ex} domains admitting approximate phase synchronization independent on the source of noise. It is interesting that each domain coincides with one of the characteristic regimes identified when discussing Fig. 5(a). In particular, at small and large τ_{ex} , there is phase synchronization between the oscillations prevailing influenced by noise, see Fig. 10(a), whereas at intermediate τ_{ex} a nearly stationary relative phase is maintained for the τ_{ex} -driven mode at both units, cf. Fig. 10(b). The actual phase shift for $\tau_{ex} < \tau_{ex}^{FC}$ is small, while for intermediate and larger τ_{ex} the units are almost perfectly synchronized in anti-phase. The source of noise is only reflected in the point that the corresponding γ values at $\tau_{ex} \approx 1$ and $\tau_{ex} \approx 2$ are slightly higher in Fig. 9(c) than in Fig. 9(a), which is a consequence of the known fact that the oscillations under optimal noise in the SISR case are more regular than those in the CR case.

For τ_{in} above τ_{in}^{FC} , there are more apparent secondary effects reflecting the external/internal character of noise. Under internal noise, an almost constant relative phase is achieved at $\tau_{ex} \approx 2$, where the prevailing behavior corresponds to a mode driven by τ_{in} . In particular, coupling delays from the interval $\tau_{ex} \in (1.9, 2.1)$ seem to affect the units' behavior in a stabilizing fashion, suppressing the noise-induced fluctuations around the typical orbit, which facilitates the establishment of a nearly stationary relative phase. One may show that the units in this domain are synchronized in anti-phase. On the other hand, the co-effects of coupling delay and external noise lead to a different picture within the interval $\tau_{ex} \in (1.6, 2.3)$. At variance with Fig. 9(b), their interplay is found to promote phase synchronization, cf. Fig. 9(d). The important contribution from the stochastic effects is corroborated by the point that the γ^{max} values in the inset of Fig. 9(d) correspond to non-negligible noise amplitudes at unit 1. Note that such D_1^1 values are not large enough to disturb the adjustment between the units' characteristic time-scales. As for the actual phase differences, around $\tau_{ex} \approx 2$ the units are approximately synchronized in anti-phase, whereas the in-phase synchronization sets in closer to the boundaries of the $\tau_{ex} \in (1.6, 2.3)$ interval.

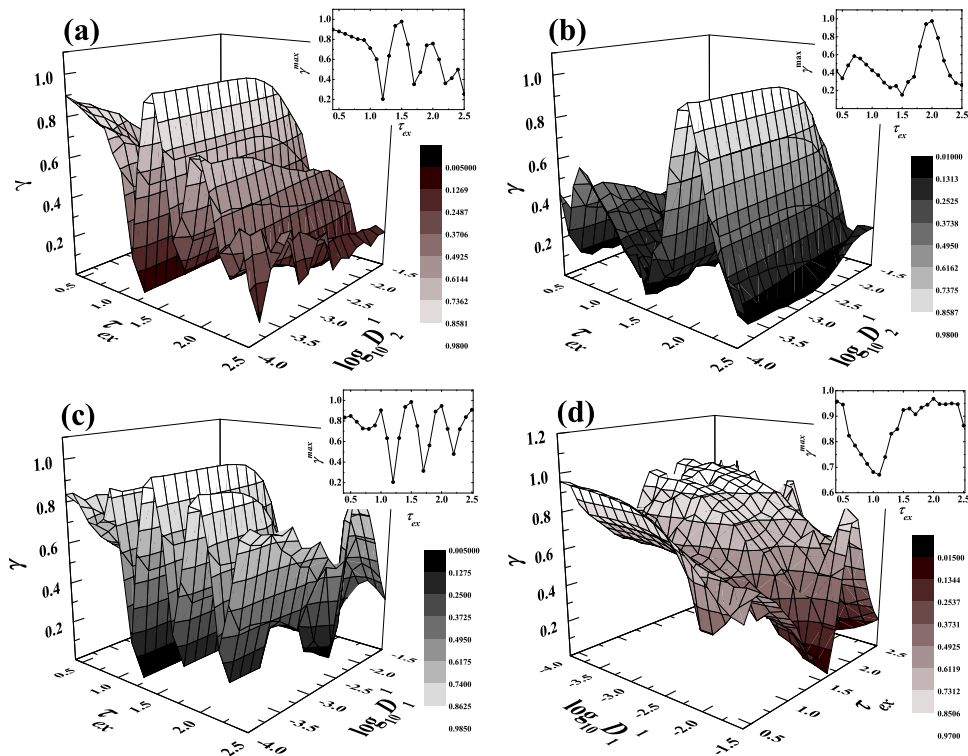


Fig. 9. The main frames display synchronization index γ as a function of τ_{ex} and noise intensity at the adjustable unit. The top (bottom) row refers to setup with internal (external) noise, whereas the left and right columns are obtained for $\tau_{in} = 0$ and $\tau_{in} = 0.4$, respectively. In the insets are shown the corresponding dependencies of the coarse-grained index γ^{max} on τ_{ex} .

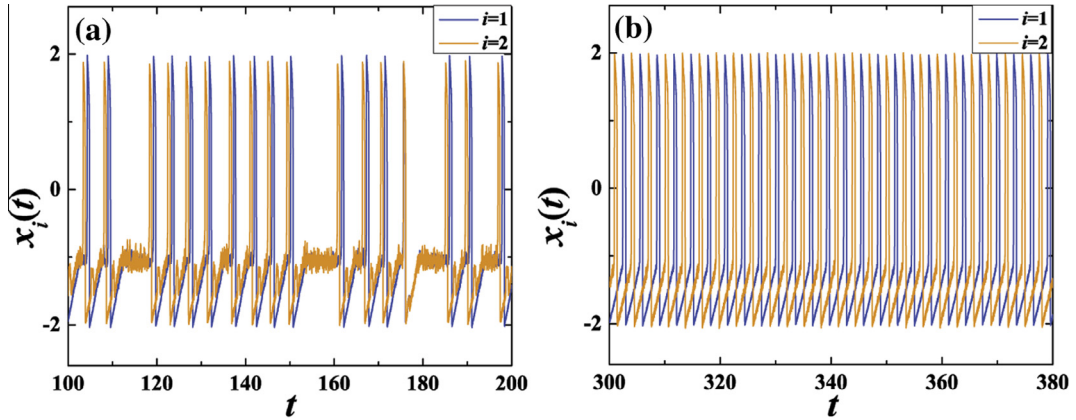


Fig. 10. (a) and (b) refer to scenarios where phase synchronization is achieved between the noise-induced oscillations and oscillations controlled by the coupling delay, respectively. $x_i(t)$ series in both cases are obtained for external noise with $\tau_{ex} = 0.9$ in (a) and $\tau_{ex} = 1.5$ in (b). Remaining parameters are $D_1^1 = 0.0002$, $D_1^2 = 0.00087$, $\tau_{in} = 0$.

6. Conclusion

In this paper, we have examined how the behavior of a typical class II excitability model is altered by incorporating an intermediate characteristic time-scale, nested between the ones defined by the activator and the recovery variable. Introduced in the FHN model, such a time-scale is associated with intrinsic delay τ_{in} , whose role is to modify the relaxation process, affecting both the declining stage of spike and the slope describing how the rest state is regained. Drawing analogy to neuroscience, the former may partly be motivated as means to approximate the gross effects of certain microscopic processes in the ion-gating channels of neuron membrane. For the paradigmatic cases, including a single unit under additive noise from external or internal sources, as well as a pair of delay-coupled noisy units, the main goal has been to understand how the competition between the noise-induced and the delay-driven (noise perturbed) oscillation modes is resolved, further considering its impact on regularity of units' firing and their synchronizability.

Given the additional ingredient in the single unit model, its stability and the onset of oscillations have been addressed in detail. Apart from carrying out the bifurcation analysis of the unperturbed system and determining the conditions for the stability of the linearized system under perturbation, we have also extended the method of statistical linearization to gain further insight into the interplay of noise and τ_{in} in light of competition between the different oscillatory modes. Regarding the role of τ_{in} , the key result on the deterministic system is that the equilibrium loses stability via the direct supercritical Hopf bifurcation at τ_{in}^H , but the unit's oscillatory motion is primarily shaped by the global fold-cycle bifurcation occurring for $\tau_{in}^{FC} < \tau_{in}^H$. In effect, a sophisticated interplay between the local and global events renders the large cycle emerging from the latter as the unique attractor already for τ_{in} slightly above τ_{in}^H . An interesting qualitative point on τ_{in} in relation to excitability is that it shifts the system away from the Hopf bifurcation controlled by b , making the unit less excitable.

Stability of the perturbed unit cannot be treated within the Fokker–Planck formalism due to inability to resolve the conditional drift term. Nevertheless, in case of the linearized system it is demonstrated that the critical τ_{in} values for the first two moments of the solutions are only marginally different, though the respective characteristic equations are distinct. Focussing on the setup admitting external noise, the method of statistical linearization has proven useful for two reasons. First, one infers that the time-averaged effect of external noise D_1 consists in suppressing the unit's excitability, quite similar to the impact of τ_{in} . The other result concerns families of curves obtained for the correlation time as a function of D_1 at different τ_{in} . These dependencies provide indirect evidence on the prevailing factor in the unit's oscillatory motion, such as the point that the τ_{in} -driven mode is strongly susceptible to external perturbation, giving way to the noise-induced mode already at intermediate D_1 .

In the noiseless case, we have shown that the system of coupled units displays bistability in most (τ_{ex}, τ_{in}) domains, which is a corollary of an intricate interplay between the local and global bifurcations. While the equilibrium undergoes a sequence of direct and inverse supercritical and subcritical Hopf bifurcations with increasing τ_{ex} at any $\tau_{in} > \tau_{in}^H$, the τ_{in} -controlled fold-cycle bifurcation inherited from the single unit is complemented by the fold-cycle bifurcation due to τ_{ex} . For any $\tau_{in} > \tau_{in}^H$, there exists a coupling delay τ_{ex} slightly smaller than the fold-cycle threshold τ_{ex}^{FC} , above which the fixed point is no longer stable. As for the oscillatory state, the large cycles elicited in global bifurcations typically survive, whereas the cycles emerging from Hopf bifurcations get annihilated in scenarios involving inverse fold-cycle bifurcation. Adding stochastic terms affects asymptotic dynamics (novel oscillatory modes, certain bistable regimes lost), but also leads to some transient phenomena (stochastic switching between oscillatory modes).

Interaction of noisy units is examined for two basic setups involving perturbation from external or internal sources. In both instances, the impact of τ_{in} is assessed by comparing two representative cases, characterized by τ_{in} lying below or above

τ_{in}^{FC} . While regularity of firing is quantified by the signal-to-noise ratio S , coordination of activities has been treated within the framework of stochastic synchronization. The latter refers to frequency synchronization, described by the ratio of average ISIs r , and the adjustment at an arbitrary moment of time, measured by the synchronization index γ .

We have numerically demonstrated that the external/internal character of noise crucially influences (i) the ability of entrainment to a single frequency and (ii) the fashion in which the competition between the delay- and noise-driven modes is resolved. Regarding (i), note that frequency synchronization turns out to be resilient against intrinsic noise, whereas it is violated by external noise if the adjustable unit is sufficiently perturbed. On the prevailing oscillatory mode, both forms of noise yield a similar paradigm for $\tau_{in} < \tau_{in}^{FC}$, whereas the differences become apparent for non-trivial $\tau_{in} > \tau_{in}^{FC}$. Below τ_{in}^{FC} , under increasing τ_{ex} the characteristic scale of oscillations is first controlled by the adjustable unit, then by the coupling delay and finally by the optimized unit. Above τ_{in}^{FC} , the scenarios with different noise terms are manifestly distinct because the τ_{in} -driven mode is more susceptible to external perturbation.

Deterministic effects due to intrinsic delay have been shown to strongly influence (i) regularity of firing and (ii) the properties of phase synchronization between the units. With respect to (i), for $\tau_{in} < \tau_{in}^{FC}$, maximal regularity reflects the onset of the fold-cycle bifurcation controlled by τ_{ex} , whereas above τ_{in}^{FC} , regularity peaks if the characteristic time-scale of the noise-induced oscillations at the optimized unit matches that of the τ_{ex} -driven mode. On (ii), note that for $\tau_{in} < \tau_{in}^{FC}$ three characteristic regimes admitting phase synchronization may be found. At small and large τ_{ex} , phase synchronization arises between the modes prevalently influenced by noise, whereas at intermediate τ_{ex} a nearly stationary relative phase is achieved for the τ_{ex} -driven modes. Above τ_{in}^{FC} , stochastic effects are more expressed under external noise, as its coaction with τ_{ex} can give rise to phase synchronization.

In this paper we have examined how introducing an intermediate characteristic time-scale affects the regularity and phase synchronization of class II excitable units subjected to external and internal sources of noise, as well as coupling delays. The fashion in which the competition between the noise-induced and delay-driven (noise-perturbed) oscillation modes is resolved can also have merit from the aspect of controlling the noise-induced oscillations through coupling delay. It would be interesting to study the similar set of issues in case of type I excitable units, represented by the Morris–Lecar model.

Acknowledgement

This work was supported in part by the Ministry of Education and Science of the Republic of Serbia, under Project Nos. 171017 and 171015.

References

- [1] Ares S, Morelli LG, Jörg DJ, Oates AC, Jülicher F. *Phys Rev Lett* 2011;106:058102.
- [2] Destexhe A, Rudolph-Lilith M. *Neuronal noise*. New York: Springer; 2012.
- [3] Sagués F, Sancho JM, García-Ojalvo J. *Rev Mod Phys* 2007;79:829.
- [4] Pedraza JM, Paulsson J. *Science* 2008;319:339.
- [5] Galla T. *Phys Rev E* 2009;80:021909.
- [6] Gupta C, Lopez JM, Ott W, Josić K, Bennett MR. *Phys Rev Lett* 2013;111:058104.
- [7] Roussel MR, Igamberdiev AU. *Biosystems* 2011;103:230.
- [8] Dhamala M, Jirsa VK, Ding M. *Phys Rev Lett* 2004;92:074104.
- [9] Popovych OV, Hauptmann C, Tass PA. *Phys Rev Lett* 2005;94:164102.
- [10] McDonnell MD, Ward LM. *Nat Rev Neurosci* 2011;12:415.
- [11] Ramana Reddy DV, Sen A, Johnson GL. *Phys Rev Lett* 1998;80:5109.
- [12] Pikovsky A, Zaikin A, de la Casa MA. *Phys Rev Lett* 2002;88:050601.
- [13] Elowitz MB, Levine AJ, Siggia ED, Swain PS. *Science* 2002;297:1183.
- [14] Raser JM, O’Shea EK. *Science* 2004;304:1811.
- [15] Blake WJ, Kaern M, Cantor CR, Collins JJ. *Nature (London)* 2003;422:633.
- [16] Gaudreault M, Drolet F, Vials J. *Phys Rev E* 2012;85:056214.
- [17] Bratsun D, Volfson D, Tsimring LS, Hasty J. *Proc Natl Acad Sci USA* 2005;102:14593.
- [18] Jia T, Kulkarni RV. *Phys Rev Lett* 2011;106:058102.
- [19] Lim J, Ryu J, Lee C, Yoo S, Jeong H, Lee J. *New J Phys* 2011;13:103002.
- [20] Izhikevich EM. *Dynamical systems in neuroscience: the geometry of excitability and bursting*. Cambridge, Massachusetts: MIT Press; 2007.
- [21] Gaudreault M, Lépine F, Vials J. *Phys Rev E* 2009;80:061920.
- [22] Gaudreault M, Berbert JM, Vials J. *Phys Rev E* 2011;83:011903.
- [23] Khovanov IA, Polovinkin AV, Luchinsky DG, McClintock PVE. *Phys Rev E* 2013;87:032116.
- [24] Muratov CB, Vanden-Eijnden E. *CHAOS* 2008;18:015111.
- [25] Zhang J, Yuan Z, Wang J, Zhou T. *Phys Rev E* 2008;77:021101.
- [26] Hauschildt B, Janson NB, Balanov A, Schöll E. *Phys Rev E* 2006;74:051906.
- [27] Burić N, Todorović D. *Phys Rev E* 2003;67:066222.
- [28] Schmid G, Goychuk I, Hänggi P. *Fluct Noise Lett* 2004;4:L33.
- [29] Brandstetter S, Dahlem MA, Schöll E. *Philos Trans R Soc A* 2010;368:391.
- [30] Pikovsky AS, Kurths J. *Phys Rev Lett* 1997;78:775.
- [31] Lee DeVille RE, Vanden-Eijnden E, Muratov CB. *Phys Rev E* 2005;72:031105.
- [32] Risken H. *The Fokker–Planck equation: methods of solutions and applications*. 2nd ed. Berlin, Heidelberg: Springer-Verlag; 1989.
- [33] Guillouzic S, L’Heureux I, Longtin A. *Phys Rev E* 1999;59:3970.
- [34] Atay FM, editor. *Complex time-delay systems: theory and applications*. Berlin, Heidelberg: Springer; 2010.
- [35] Campbell SA. Time delays in neural systems. In: McIntosh R, Jirsa VK, editors. *Handbook of brain connectivity*. Berlin, Heidelberg: Springer-Verlag; 2007. p. 65–90.

- [36] Campbell SA. Calculating centre manifolds for delay differential equations using Maple. In: Balachandran B, Kalmar-Nagy T, Gilsinn D, editors. Delay differential equations: recent advances and new directions. New York: Springer-Verlag; 2009. p. 221–45.
- [37] Mackey MC, Nechaeva IG. Phys Rev E 1995;52:3366.
- [38] Lei J, Mackey MC. SIAM J Appl Math 2007;67:387.
- [39] Pomplun J, Amann A, Schöll E. EuroPhys Lett 2005;71:366.
- [40] Kottalam J, Lindenberg K, West BJ. J Stat Phys 1986;42:979.
- [41] Lindner B, Garcia-Ojalvo J, Neiman A, Schimansky-Geier L. Phys Rep 2004;392:321.
- [42] Zaks MA, Neiman AB, Feistel S, Schimansky-Geier L. Phys Rev E 2003;68:066206.
- [43] Franović I, Todorović K, Vasović N, Burić N. Phys Rev E 2013;87:012922.
- [44] Franović I, Todorović K, Vasović N, Burić N. Phys Rev Lett 2012;108:094101.
- [45] Hasegawa H. Phys Rev E 2004;70:021911.
- [46] Gardiner CW. Handbook of stochastic methods for physics, chemistry and the natural sciences. 3rd ed. Berlin, Heidelberg: Springer-Verlag; 2004.
- [47] Engelborghs K, Luzyanina T, Samaey G. Technical report TW-330, Department of Computer Science, K.U. Leuven Leuven, Belgium; 2001.
- [48] Engelborghs K, Luzyanina T, Roose D. ACM Trans Math Softw 2002;28:1.
- [49] Wiggins S. Introduction to applied nonlinear dynamical systems and chaos. 2nd ed. New York, Cambridge: Springer; 2000.
- [50] Hu B, Zhou C. Phys Rev E 2000;61:R1001.
- [51] Pei X, Wilkens L, Moss F. Phys Rev Lett 1996;77:4679.
- [52] Neiman A, Silchenko A, Anishchenko V, Schimansky-Geier L. Phys Rev E 1998;58:7118.
- [53] Rosenblum M, Pikovsky A, Kurths J, Schäfer C, Tass PA. Phase synchronization: from theory to data analysis. In: Moss F, Gielen S, editors. Neuroinformatics and neural modelling. Amsterdam, The Netherlands: North-Holland; 2001. p. 279–322.